Published in final edited form as:
J Am Chem Soc. 2006 February 1; 128(4): 1293–1303. doi:10.1021/ja056528r.

Alkaline Phosphatase Mono- and Di-esterase Reactions: Comparative Transition State Analysis

Jesse G. Zalatan† and **Daniel Herschlag***,†,‡

† *Department of Chemistry, Stanford University, Stanford, CA 94305*

‡ *Department of Biochemistry, Beckman Center B400, Stanford University, Stanford CA 94305*

Abstract

Enzyme-catalyzed phosphoryl transfer reactions have frequently been suggested to proceed through transition states that are altered from their solution counterparts. Previous work with *E. coli* alkaline phosphatase (AP), however, suggests that this enzyme catalyzes the hydrolysis of phosphate monoesters through a loose, dissociative transition state, similar to that in solution. AP also exhibits catalytic promiscuity, with a low level of phosphodiesterase activity, despite the tighter, more associative transition state for phosphate diester hydrolysis in solution. Because AP is evolutionarily optimized for phosphate monoester hydrolysis, it is possible that the active site environment alters the transition state for diester hydrolysis to be looser in its bonding to the incoming and outgoing groups. To test this possibility, we have measured the non-enzymatic and AP-catalyzed rate of reaction for a series of substituted methyl phenyl phosphate diesters. The values of β_{lg} and additional data suggest that the transition state for AP-catalyzed phosphate diester hydrolysis is indistinguishable from that in solution. Instead of altering transition state structure, AP catalyzes phosphoryl transfer reactions by recognizing and stabilizing transition states similar to those in aqueous solution. The AP active site therefore has the ability to recognize different transition states, a property that could assist in the evolutionary optimization of promiscuous activities.

Introduction

E. coli alkaline phosphatase (AP) catalyzes the hydrolysis of a broad range of phosphate monoester substrates, presumably to harvest phosphate for nucleic acids and various metabolites.[1] AP also catalyzes phosphate diester hydrolysis.[2] The 10^{11}-fold overall rate enhancement for enzymatic diester hydrolysis relative to the solution reaction is substantial, but small in comparison with the $>10^{17}$-fold rate enhancement for monoester hydrolysis. The catalytic promiscuity of AP and other enzymes supports a model for enzyme evolution in which enzymes that can catalyze alternative reactions with a low level of activity will have a selective advantage for evolutionary optimization of that activity, subsequent to a gene duplication event.[3-8] Furthermore, the existence of evolutionarily related homologs of AP that preferentially catalyze phosphate diester hydrolysis implies that the phosphodiesterase activity of AP can be optimized to levels that are reasonable for biological function.[9-11]

The AP active site contains two Zn^{2+} ions and an arginine residue that are positioned to interact with the substrate, and a serine alkoxide that displaces the leaving group in the first step of the

* To whom correspondence should be addressed. E-mail: herschla@cmgm.stanford.edu..

Supporting Information Available. Data compiled from the literature for non-enzymatic LFERS with 4-nitro and 4-cyano phenyl leaving groups, plots of the log of the rate constant for the AP-catalyzed reactions of phosphate diesters and phenyl sulfates versus that for the corresponding phenyl phosphorothioates, and NMR chemical shift data for methyl phenyl phosphate diesters. This material is available free of charge via the Internet at http://pubs.acs.org.

reaction to produce a covalent enzyme-phosphate intermediate (Scheme 1A).[12, 13] This intermediate is subsequently hydrolyzed by water in the second step of the reaction.[1] It has been proposed that active sites containing two metal ions are well-suited for catalyzing phosphoryl transfer reactions of both monoesters and diesters.[14, 15] In the simplest case, one metal ion activates the incoming nucleophile and another metal ion stabilizes charge buildup on the leaving group oxygen, as proposed for AP-catalyzed phosphate monoester hydrolysis (Scheme 1A). This mechanism is very similar to that proposed for phosphate diester hydrolysis catalyzed by Klenow exonuclease and other phosphodiesterases,[14, 16, 17] raising an important question: how do these active sites distinguish between different types of phosphate ester substrates? These distinctions are especially important for understanding how a two metal ion phosphate monoesterase could evolve into a diesterase or *vice versa*.

According to transition state theory, enzymatic rate enhancements arise from preferential stabilization of the transition state relative to the ground state.[18-22] Consequently, the specificity of an enzyme for a particular reaction depends on its ability to recognize and stabilize the transition state for that reaction, and characterization of the structure of the transition state is a critical step towards understanding both how enzymes catalyze reactions in general and how they distinguish between different reactions. We sought to characterize the transition state for AP-catalyzed phosphate diester hydrolysis for comparison with previous characterizations of the transition state for AP-catalyzed phosphate monoester hydrolysis.[23-28] Phosphate monoesters and diesters proceed through different transition states in solution, raising the possibility that AP alters the transition state for phosphate diester hydrolysis to resemble that for phosphate monoesters.

Phosphate monoester hydrolysis in solution proceeds through a loose transition state, with nearly complete bond cleavage to the leaving group and little bond formation to the nucleophile (Scheme 2A).[29-33] In contrast, phosphate diester hydrolysis in solution proceeds through a tighter transition state than that for monoesters (Scheme 2B).[33-37] These transition states can be considered in the context of two limiting extremes. In the dissociative limit, there is complete bond cleavage to the leaving group and no bond formation to the nucleophile. In the associative limit, there is no bond cleavage to the leaving group and complete bond formation to the nucleophile.[33] A transition state that is close to the dissociative limit is “loose,” while a transition state that is close to the associative limit is “tight.” A transition state that is midway between loose and tight is referred to as “synchronous” herein, as the reaction can be considered to occur with the extent of bond breaking to the outgoing group reflecting the extent of bond making to the incoming group such that the sum of the axial bond orders is approximately one.

The positions of the transition states for the solution reactions of phosphate monoesters and diesters relative to the limiting extremes are represented on two-dimensional reaction coordinate diagrams, or More-O'Ferrall-Jencks diagrams,[38, 39] in Figure 1A and B. The reactants and products are located in the lower left and upper right corners, respectively, and the remaining corners are the dissociative and associative limits. The two-dimensional reaction coordinate defines a three-dimensional free energy surface in which free energy axis is perpendicular to the page. The reactants and products are in free energy wells. The transition state is located at a saddle point on the free energy surface. It is a maximum along the path from reactants to products but a minimum along the “tightness coordinate,” the line connecting the dissociative and associative limits. The transition state for phosphate monoester hydrolysis is located close to the dissociative limit (Figure 1A), whereas the transition state for phosphate diester hydrolysis is synchronous, roughly midway between the extremes (Figure 1B). In the case of formation of a stable intermediate, an additional free energy well could occur in the dissociative or associative corner.

Results from initial experiments using both thio-effects and linear free energy relationships (LFERs) to characterize the transition state for AP-catalyzed monoester hydrolysis were interpreted in terms of a transition state that was tighter than that for the solution reaction.[40-42] The apparent change in the nature of the transition state was attributed to electrophilic interactions in the enzyme active site. It was later determined that the LFER experiments were conducted either in conditions under which the chemical step was not rate limiting or in the presence of inhibitory concentrations of inorganic phosphate.[27] Furthermore, thio-effects in enzymatic reactions are not as simply interpreted as those in solution reactions due to effects on binding interactions within the active site that can mask effects arising from the nature of the transition state.[24, 44-46] Subsequent experiments provided strong evidence for a loose enzymatic transition state similar to that in solution and suggested that electrostatic interactions in the active site do not alter the nature of the transition state.[23-28]

Although phosphate diester hydrolysis in solution proceeds through a synchronous transition state that is tighter than that for monoesters (Scheme 2), the AP active site is optimized for phosphate monoester hydrolysis through a loose transition state. There are two general models for how AP can catalyze phosphate diester hydrolysis. First, the AP active site might favor a looser transition state for diester hydrolysis relative to the reaction in solution. Alternatively, AP could be capable of recognizing and stabilizing a synchronous diester transition state similar to that in solution. Figure 1C and D depict these possibilities on cross sections of the free energy surface along the tightness coordinate. The nature of the transition state for the enzyme catalyzed reaction depends both on the specificity of the active site for a particular transition state and the steepness of the "intrinsic" free energy surface. An active site that is highly specific for loose transition states would favor a looser transition state for enzymatic phosphate diester hydrolysis, while an active site that is capable of stabilizing a tighter transition state would favor a synchronous enzymatic transition state. The steepness of the intrinsic free energy surface determines how energetically costly it is to vary the extent of bonding in the transition state (Figure 2). If the energy well at the transition state is shallow, there is little energetic cost to shifting the nature of the transition state. If the energy well is steep, there will be a significant energetic cost associated with shifting the transition state, and with a sufficiently steep energy well even an active site that is highly specific for loose transition states would be unable to significantly alter the transition state for diester hydrolysis relative to that in solution.

The results described herein suggest that the AP-catalyzed phosphate diester hydrolysis reaction proceeds through a synchronous transition state, indistinguishable from diester hydrolysis in solution. The same bimetallo active site therefore has the ability to recognize both the loose transition state for phosphate monoester hydrolysis and the synchronous transition state for phosphate diester hydrolysis. This flexibility could have assisted in the evolution of a phosphodiesterase on the AP scaffold.

Results and Discussion

To characterize the transition state for AP-catalyzed phosphate diester hydrolysis, we compared enzymatic and non-enzymatic linear free energy relationships (LFERs) for phosphate diester hydrolysis. LFERs are a powerful tool for characterization of transition state structure.[22, 47] The slope of the line correlating the log of the rate constant with the pK_a of the leaving group (the Brønsted coefficient, β_{lg}) measures the sensitivity of the transition state to charge buildup at the position of bond cleavage and reflects the extent of bond cleavage in the transition state.[48]

The LFER approach requires the use of a series of homologous compounds with leaving groups of varying pK_a. While this approach is highly effective for characterizing solution reactions, enzymatic reactions can be complicated by specific enzyme-substrate interactions. However,

the existence of an open binding site without specific leaving group interactions[12] and the use of a large set of homologous compounds has allowed the applications of LFERs to the AP-catalyzed hydrolysis of phosphate monoesters,[25, 27] phosphorothioate monoesters,[24, 26] and sulfate monoesters.[28] In each case, the LFERs suggested a loose transition state structure, and these compounds all react via loose transition states in solution. In the previous work, as with the experiments described here, only the extent of bonding to the leaving group in the transition state was measured. The absence of an observed change in bonding to the leaving group in the previous and current work suggests, most simply, that bonding to the nucleophile is also unaffected in the enzymatic transition state relative to that in solution.

Non-enzymatic Hydrolysis of Methyl Phenyl Phosphate Diesters

Values of β_{lg} reported in the literature for the solution reactions of phosphate diesters range from −0.64 to −0.97 and support the general conclusion that the transition state is roughly synchronous.[35, 49-52] These studies, however, employed limited sets of compounds, included ortho-substituted compounds, or included a rate constant for the slow reaction of dimethyl phosphate that was later determined to be an overestimate.[53] We therefore obtained a value of β_{lg} for the non-enzymatic reaction of a series of methyl phenyl phosphate diesters (Scheme 3) with hydroxide ion for comparison to the enzymatic results with the same series of compounds.

Second-order rate constants for the reaction of hydroxide with the series of methyl phenyl phosphate diesters are reported in Table 1. Figure 3 shows the dependence of $\log(k_{HO^-})$ on leaving group pK_a and gives a value of β_{lg} of −0.94 ± 0.05. The parameter β_{lg}/β_{eq} represents the fractional effective charge in the transition state, where β_{eq} is the dependence of $\log(K_{eq})$ on leaving group pK_a.[54, 55] Using −1.73 as an estimate of β_{eq} for substituted phenyl phosphate diesters[56] gives a fractional effective charge of 0.5, consistent with a synchronous transition state. For comparison, the fractional effective charge in the loose transition state for phosphate monoester hydrolysis is 0.9, estimated from the values of β_{lg} and β_{eq} of −1.23 and −1.35, respectively.[30, 56]

Rate constants for 4-nitro and 4-cyano phenyl substituted phosphate diesters were not included in the fit used to determine the value of β_{lg}. There are several examples in the literature of deviations of compounds with 4-nitro or 4-cyano phenyl substituents from solution LFERS, presumably due to resonance effects (see Supporting Information). Furthermore, compounds with 4-nitro and 4-cyano phenyl substituents are unambiguous outliers from LFERs for AP-catalyzed hydrolysis reactions.[24, 26, 28] However, inclusion of these points in the LFERs for both non-enzymatic and enzymatic reactions does not affect the conclusions drawn from the comparison to the AP-catalyzed reaction.

Enzymatic Hydrolysis of Methyl Phenyl Phosphate Diesters

The products of methyl phenyl phosphate diester hydrolysis are a substituted phenol and methyl phosphate, but because AP is a proficient monoesterase, the methyl phosphate product is rapidly hydrolyzed to inorganic phosphate (P_i) and methanol. To avoid inhibition by P_i, the AP-catalyzed hydrolysis rates of a series of phosphate diesters were determined with an AP variant in which Arg166 was mutated to Ser (Scheme 1B). P_i binds wild type (wt) AP with an affinity of ~1 μM, which creates serious complications for kinetic assays that have detection limits in this concentration range.[27] P_i binds R166S AP with an affinity of 420 μM,[2, 59] allowing kinetic assays to be performed under conditions such that the P_i concentration is well below inhibitory levels.

Mutation of Arg166 to Ser does not alter the reactivity of AP with phosphate diesters, presumably because the arginine side chain can readily flip out of the active site to allow

phosphate diester binding.[2] Furthermore, Arg166 does not have a significant effect on LFERs for AP-catalyzed hydrolysis reactions; the values of β_{lg} for hydrolysis of phosphate and phosphorothioate monoesters are similar upon mutation of Arg166.[25, 26] These properties render R166S AP ideally suited for studies on the AP-catalyzed phosphate diester hydrolysis reaction.

The values of k_{cat}/K_M for R166S AP-catalyzed hydrolysis of methyl phenyl phosphate diesters are reported in Table 1. Figure 4 shows the leaving group dependence of $\log(k_{cat}/K_M)$, which gives a β_{lg} value of −0.95 ± 0.08. Compounds with 4-nitro and 4-cyano phenyl leaving groups were omitted from the fit as discussed below.

β_{lg} measures the sensitivity of the transition state to charge buildup at the leaving group oxygen and can be affected by interactions with the local environment. Therefore, to compare the enzymatic value of β_{lg} to that obtained for the solution hydrolysis reaction, binding interactions with the active site Zn^{2+} ions must be taken into account. Furthermore, the appropriate solution reference reaction for comparison to the enzymatic reaction is one with a nucleophile of comparable strength to the enzymatic nucleophile. These effects are accounted for as described in the Methods section and used to predict values of β_{lg}^{obs} for hypothetical loose, synchronous, and tight enzymatic transition states based on the known values of β_{lg} for solution reactions of phosphate monoesters, diesters, and triesters respectively (Table 2).

The following comparisons suggest that the observed value of β_{lg} of −0.95 ± 0.08 corresponds to a synchronous transition state, similar to that for reactions of phosphate diesters in solution. For a synchronous enzymatic transition state analogous to diester hydrolysis in solution, the value of β_{lg}^{obs} is predicted to be −0.85. For a loose, monoester-like transition state, the value of β_{lg}^{obs} is predicted to be −1.11, and for a tight, triester-like transition state, the value of β_{lg}^{obs} is predicted to be −0.43. The observed value of −0.95 ± 0.08 for AP-catalyzed phosphate diester hydrolysis is closest to that predicted for the synchronous transition state. There is, however, significant uncertainty in the predicted values of β_{lg}^{obs}, due to assumptions required about the effects of the interactions between the active site Zn^{2+} ions and the transition state (see Methods), and the observed value lies between the values predicted for synchronous and loose transition states. For AP-catalyzed phosphate monoester hydrolysis, the predicted value of β_{lg}^{obs} is −0.69, smaller in magnitude than the observed value of −0.85.[27] The transition state for phosphate monoester hydrolysis in solution is close to the dissociative limit, and it is unlikely that the transition state for AP-catalyzed hydrolysis is looser than that in solution. Instead, the predictions probably overestimate the effects that reduce the magnitude of β_{lg}^{obs} (Table 2). These comparisons suggest that the observed value of −0.95 ± 0.08 for AP-catalyzed phosphate diester hydrolysis corresponds to an approximately synchronous transition state, similar to that in solution. Nevertheless, the predicted values of β_{lg} are based on the behavior of model compounds in solution and we do not know how accurate these models are in describing interactions in the AP active site. Thus, we cannot estimate uncertainties in the predicted values of β_{lg} and a shift to a looser transition state cannot be excluded based solely on comparisons of the predicted and observed values of β_{lg}. However, the following analysis of outliers from LFERs provides strong evidence supporting a more synchronous transition state for phosphate diesters than phosphate monoesters.

Compounds with 4-nitro and 4-cyano phenyl leaving groups are outliers from LFERs in several non-enzymatic reactions (see Supporting Information) and in AP-catalyzed hydrolysis reactions.[24, 26, 28] In a plot of the log of the rate constant for the AP-catalyzed reactions of phenyl sulfates versus that for the corresponding phenyl phosphorothioates, the 4-nitro and 4-

cyano outliers fall on the same correlation line as the other leaving groups in the series, demonstrating that the magnitudes of the deviations are the same for both reactions. This observation is consistent with the conclusion that sulfate and phosphorothioate monoesters proceed through similar loose transition states with extensive charge buildup on the phenolate oxygen.[28] In contrast, the magnitudes of the deviations of 4-nitro and 4-cyano phenyl leaving groups from the diester LFER are smaller than observed for the phosphorothioate or sulfate reactions (Figure 5 and Figure S9 in Supporting Information).

Two simple models that can account for the smaller deviations both suggest a transition state for AP-catalyzed diester hydrolysis that is tighter than for monoester hydrolysis. Evidence against alternative models is presented below. In model I, deviations from LFERs arise if resonance delocalization lags behind charge buildup (i.e., non-perfect synchronization) such that the leaving group pK_a overestimates the ability of a substituent to stabilize charge buildup in the transition state.[60] The lack of resonance stabilization in the transition state would be more unfavorable for transition states with increased charge buildup, leading to larger deviations for reactions with looser transition states. In model II, deviations arise if resonance delocalization affects interactions with the active site Zn^{2+}. These active site interactions are likely to be strong in loose transition states with extensive charge buildup at the phenolate oxygen. Resonance delocalization of charge could weaken interactions with the Zn^{2+}, leading to slower reactions than would be predicted from the leaving group pK_a (Figure 6A and B). In a tighter transition state, there is less total charge buildup at the phenolate oxygen, which results in a weaker interaction with the active site Zn^{2+} and a correspondingly smaller deviation due to resonance delocalization (Figure 6C and D). Each of the models described above supports the conclusion that the transition state for AP-catalyzed phosphate diester hydrolysis is synchronous.

Alternative models to account for the deviations have been considered and ruled out as follows. A change in the rate-determining step can be ruled out based on the substantially faster hydrolysis rates of 3,4-dinitrophenyl phosphorothioate (leaving group pK_a 5.4) and methyl 2,4-dinitrophenyl phosphate (leaving group pK_a 4.1) relative to the respective 4-nitro analogs.[2, 24] A specific, detrimental interaction with the AP active site could lead to deviations for bulky groups at the *para* position. However, this putative interaction would have been expected to lead to a similar deviation for methyl phenyl phosphate diesters as was observed for phenyl phosphorothioates and sulfates. Finally, Arg166 could play a role in the deviations, as LFERs for AP-catalyzed phenyl phosphorothioate and phenyl sulfate hydrolysis reactions were obtained with wt AP, but the LFER for AP-catalyzed phosphate diester hydrolysis was obtained with R166S AP. Removal of Arg166 has no significant effect on the magnitude of the deviations for phenyl phosphorothioate hydrolysis,[26] rendering this model unlikely. Nevertheless, the possibility of a more complex model in which the absence of Arg166 alters the binding modes for methyl phenyl phosphate diesters cannot be completely eliminated.

Implications for the Nature of the Transition State for Enzymatic Phosphoryl Transfer Reactions

There have been many suggestions that enzymatic phosphoryl transfer reactions proceed through transition states that are altered from their solution counterparts.[61] These proposals are often based on the expectation that for loose transition states, the non-bridging phosphate ester oxygen atoms must donate negative charge to phosphorus to compensate for the loss of bonding to the incoming and outgoing groups. For tight transition states, negative charge is expected to build up on the non-bridging atoms as bonding to the incoming group increases. Positively charged functional groups in enzyme active sites would then favor an increase in negative charge buildup on the non-bridging atoms in the transition state and thus a tighter transition state. However, if the free energy well along the tightness coordinate at the transition

state is sufficiently steep, then positively charged active site functional groups would not provide a sufficient driving force to significantly alter the transition state. (Figure 2 depicts this effect for an enzymatic transition state that is looser than the solution transition state; the same considerations apply for a tighter transition state). Furthermore, the charge distribution on the non-bridging atoms in a loose or tight transition state has not been determined experimentally. Computational studies on metaphosphate monoanion suggest that charge remains localized on the non-bridging atoms.[62, 63] Thus, there may be significant negative charge on the non-bridging atoms in a loose transition state and interactions with positively charged functional groups in enzyme active sites do not necessarily favor a tighter transition state.

It has also been suggested that the distance between the two metals ions in the AP active site corresponds to the distance between the entering and leaving groups in the transition state and is predictive of the nature of the enzymatic transition state.[64] However, the results described herein suggest that AP catalyzes reactions with phosphate monoesters and diesters through transition states that have different amounts of bonding to the axial groups with the same Zn^{2+}-Zn^{2+} distance. Nevertheless, it is possible that different Zn^{2+}-Zn^{2+} distances lead to preferential catalysis of different reactions. Also, the AP active site may allow some motion of the bound Zn^{2+} ions, and different microstates may be more adept at catalyzing reactions of different substrates.

A growing body of experimental results from LFER and kinetic isotope effect (KIE) studies suggests that enzyme-catalyzed phosphoryl transfer reactions generally proceed through transition states that are similar to their respective solution transition states. For example, phosphate monoesters have been suggested to proceed through loose, solution-like transition states in the reactions catalyzed by protein tyrosine phosphatases,[65-67] serine/threonine protein phosphatases,[68, 69] GTPases,[70] protein tyrosine kinases,[71, 72] and acylphosphatases.[73] Phosphate diesters have been suggested to proceed through synchronous transition states in the reactions catalyzed by kanamycin nucleotidyltransferase[74] and the ribonuclease P ribozyme.[75] Diester hydrolysis catalyzed by phosphodiesterase I was also suggested to proceed through a synchronous transition state, but with protonation of a nonbridging oxygen based on the relatively large inverse nonbridging KIEs.[37] The results of subsequent KIE studies of other enzyme-catalyzed phosphoryl transfer reactions, however, suggest that these results could be a consequence of active site metal ion interactions rather than protonation.[68]

KIE studies of the reaction catalyzed by phosphotriesterase also suggest a transition state similar to that in solution,[76] although there are some distinguishing features of the enzymatic reaction. The primary KIE for enzymatic *O*,*O*-diethyl *O*-(4-carbamoylphenyl) phosphate hydrolysis is larger than that for alkaline hydrolysis.[76] Similarly, values of β_{lg} are more negative than those for solution reactions.[77, 78] These results were suggested to reflect increased cleavage of the leaving group bond in the transition state, and could be caused in part by presence of the weaker enzymatic nucleophile relative to hydroxide ion in solution.[79] However, the values of β_{lg} for some metal-substituted variants of phosphotriesterase are significantly more negative than the value of β_{eq},[78] which in principle represents the limiting value for full bond cleavage. These results are difficult to account for and may reflect negative charge buildup in a hydrophobic active site environment.[76]

Results from recent structural studies suggest a different picture may hold for some enzymes. The interconversion of phosphoenolpyruvate and phosphonopyruvate catalyzed by phosphoenolpyruvate mutase has been suggested to proceed via a fully dissociative mechanism with a metaphosphate intermediate based on the retention of stereochemistry of the reaction and the apparent lack of an enzymatic nucleophile that would enable a double displacement mechanism.[80] The presence of metaphosphate was suggested from the crystal structure of

fructose-1,6-bisphosphatase,[81] and phosphorane intermediates were suggested from the crystal structures of β-phosphoglucomutase[82] and phospholipase D,[83] although the β-phosphoglucomutase case in particular remains controversial.[84-88] These results have been suggested to support reaction mechanisms that proceed through formal intermediates instead of a concerted mechanism through a single transition state. Some enzymatic glycosyl transfer reactions have been suggested to proceed through oxycarbenium intermediates, whereas most proceed through loose, oxycarbenium-like transition states without an intermediate.[89, 90] Related solution reactions can also proceed with or without the formation of a discrete oxycarbenium intermediate.[91, 92]

The suggestion that the transition states for several enzymatic phosphoryl transfer reactions are similar to their solution counterparts is consistent with the expectation that less energy is required to stabilize a solution-like transition state than a substantially altered transition state (see Figure 1 C, D; $|\Delta\Delta G_1^{\ddagger}| > |\Delta\Delta G_2^{\ddagger}|$). The data obtained in this work suggests that even an active site that is optimized for a loose transition state does not alter the transition state for a reaction that proceeds through a tighter transition state in solution. Nevertheless, there may be situations in which the transition state structure diverges substantially from that observed in solution. The active site features that might lead to such departures are not yet understood.

Implications for Catalysis and Evolution

AP-catalyzed phosphate monoester hydrolysis proceeds through a loose transition state with a $>10^{17}$-fold rate enhancement, while phosphate diester hydrolysis proceeds through a tighter, synchronous transition state with a 10^{11}-fold rate enhancement.[2] The smaller rate enhancement for diester hydrolysis indicates that the AP active site binds the synchronous transition state for diester hydrolysis transition state more weakly than it binds the loose transition state for monoester hydrolysis and suggests that the looseness or tightness of the transition state could account for the different rate enhancements. Other features of the transition state, however, must also be important for determining the rate enhancement for AP-catalyzed reactions. AP-catalyzed sulfate monoester hydrolysis proceeds through a loose transition state similar to phosphate monoester hydrolysis, but with a rate enhancement of only 10^9-fold.[93]

Additional active site interactions can contribute to discrimination between phosphate monoester and diester substrates. Mutation of Arg166 to Ser leads to a 10^4-fold decrease in k_{cat}/K_M for phosphate monoesters[25] but does not affect the rates of phosphate diester reactions,[2] suggesting that this residue is important for binding and positioning of monoester substrates. To optimize diesterase activity on the AP scaffold, binding interactions with the diester functionality on the transferred phosphoryl group (R' in Scheme 1B) could be introduced to assist with specific binding and positioning of diester substrates.

Electrostatic properties of the non-bridging phosphate ester oxygen atoms and their interactions with the bimetallo center have also been suggested to be important. The rate enhancements for R166S AP-catalyzed hydrolysis reactions correlates with the amount of negative charge situated between the two Zn^{2+} ions in the AP active site, suggesting that these electrostatic interactions make a large contribution to catalysis.[94] Nevertheless, there are many examples of binuclear metalloenzymes that preferentially hydrolyze phosphate diesters.[16, 17] Thus, the presence of two closely spaced divalent cations does not necessarily lead to preferential monoester hydrolysis. As noted above, diester hydrolysis could be favored by binding interactions with the transferred substituent that is absent on a monoester substrate (R' in Scheme 1B). However, it is also possible that active site features tune the electrostatic properties of the bimetallo cluster by varying the coordinating ligands, the spacing between the metal ions, or the presence or absence of other nearby charged groups to favor reactions of monoesters or diesters.

We now consider evolutionary scenarios in which a diesterase evolved from AP; the same considerations apply if AP were to have evolved from a diesterase. If AP-catalyzed phosphate diester hydrolysis proceeded through a loose, monoester-like transition state, then evolution of a diesterase might have involved shifting the transition state back to a synchronous, solution-like transition state. Such a change could have played an important role in optimization of catalysis, as less energy is required to stabilize a solution-like transition state than a substantially altered transition state. Alternatively, a scenario in which other mechanisms were employed to provide greater stabilization of a looser transition state for the diesterase reaction (increasing $|\Delta\Delta G_1^{\ddagger}|$ in Figure 1C) might have been possible. These evolutionary scenarios, however, can be ruled out by the observation that the phosphate diester hydrolysis reaction catalyzed by AP already proceeds through a synchronous transition state. Optimization of this activity then simply requires improved binding of the synchronous transition state (increasing $|\Delta\Delta G_2^{\ddagger}|$ in Figure 1D).

Conclusions and Future Directions

The results described herein suggest that AP catalyzes phosphate diester hydrolysis through a synchronous transition state that is indistinguishable from that in solution, even though the AP active site is optimized for the loose transition state of the phosphate monoester hydrolysis reaction. Thus, evolution of a proficient phosphodiesterase on the AP-scaffold could occur without the need to alter the transition state structure. It will be fascinating to compare the AP active site to homologous active sites that preferentially catalyze phosphate diester hydrolysis. Determining the physical changes that have occurred in the AP active site to optimize phosphodiesterase activity will improve our understanding of the catalytic mechanisms of this important class of enzymes, provide insight into how new enzyme activities evolve, and assist in the engineering of artificial enzymes.

Materials and Methods

Materials

The plasmid for expression of R166S AP (pEK1152) and the phoA$^-$ strain of *E. coli* (SM547) were provided by Evan Kantrowitz.[59] HPLC grade acetone was used for synthesis without distillation.

Synthesis of Methyl Phenyl Phosphate Diesters

Lithium salts of methyl phenyl phosphate diesters where prepared as described[52] except that the reflux step was extended to two hours and the product was purified on silica gel using ethyl acetate/hexanes/methanol in a gradient from (20:80:0) to (20:60:20) instead of recrystallization. Yields averaged ~25%. Purified products were characterized by ^{1}H and ^{31}P NMR on a Varian Mercury 400 MHz instrument in D_2O solvent. NMR chemical shift data are reported in Supporting Information.

Non-enzymatic Phosphate Diester Hydrolysis Kinetics

Reactions of hydroxide ion with phosphate diesters were performed at 42 °C and ionic strength was adjusted to 1.0 with NaCl. Absorbance of the phenolate ion product was monitored continuously using a Uvikon 9310 spectrophotometer at the following wavelengths: 4-nitro (400 nm), 4-chloro-3-nitro (400 nm), 4-cyano (274 nm), 3-nitro (390 nm), 3,4-dichloro (302 nm), 3-chloro (291 nm), 3-fluoro (282 nm), 4-chloro (296 nm), 4-fluoro (297 nm), and parent (286 nm). Bimolecular rate constants were obtained from initial rates (≤2% reaction). Reactions were shown to be first order in hydroxide ion from 0.05 to 0.5 M and in phosphate diester over a 10-fold concentration range (between the limits of 0.1 and 10 mM). The first order

dependence on hydroxide ion concentration demonstrates that the phosphate diester monoanion is the reactive species. Under these conditions, direct attack by hydroxide at phosphorus is the dominant reaction.[95] Two alternative reaction possibilities can be ruled out as follows. First, isotope incorporation studies rule out nucleophilic aromatic substitution by attack at the phenolic carbon of the leaving group.[36] Second, hydroxide attack at the methyl carbon followed by subsequent hydrolysis of a phosphate monoester can be ruled out because phosphate monoester hydrolysis, which would be required to give the phenolate and the observed increase in absorbance, is too slow to account for the observed reaction rates.[30, 96]

Alkaline Phosphatase Purification

R166S alkaline phosphatase was purified as previously described,[2] except that the dialysis step was omitted. Protein concentration was determined by absorbance at 280 nm (ε_{280} = 3.14 × 10^4 $M^{-1}cm^{-1}$ in monomer units).[97] Concentrations determined by activity assays using 1 mM PNPP agreed to within 20% (k_{cat} = 0.44 s^{-1}).[59]

Enzymatic Phosphate Diester Hydrolysis Kinetics

Reactions were performed with 0.1 M NaMOPS pH 8.0, 0.5 M NaCl, 1 mM $MgCl_2$, and 0.1 mM $ZnSO_4$ at 25 °C. Appearance of phenolate was monitored by removing aliquots from the reaction, quenching in an equal volume of 0.1 M NaOH, and measuring the absorbance using a Uvikon 9310 at the wavelengths listed above. Rate constants were obtained from initial rates (≤2% reaction). Reactions were shown to be first order in substrate and enzyme by varying substrate concentration over a 10-fold range (between the limits of 0.1 and 10 mM) and enzyme concentration from 1 to 10 μM. Apparent second order rate constants k_{cat}/K_M are reported per active site. For 4-nitro, 4-chloro-3-nitro, 4-cyano, 3-nitro, and 3,4-dichloro substrates, rates constants were also determined independently by monitoring phenolate absorbance continuously at pH 8.0, and the rate constants agreed with those from the quench assay to within 2% in side-by-side comparisons.

To confirm that the observed diesterase activity was due to R166S AP and not contamination by a small quantity of a proficient diesterase, the inhibition constant for P_i was measured with PNPP, a phosphate monoester, and several phosphate diester substrates. The values of the inhibition constant for the monoester and diester reactions agreed to within 10% (data not shown), strongly suggesting that the monoesterase and diesterase reactions occurred in the same active site in R166S AP.[2]

Comparison of AP-catalyzed and Non-enzymatic Values of β_{lg} for a Diester-like Transition State

Comparison of β_{lg} between solution and enzymatic reactions was undertaken following a previously described approach for AP-catalyzed reactions.[27] Binding interactions with the active site Zn^{2+} (Scheme 4) and changing the nucleophile strength are expected to affect the observed value of β_{lg} according to:

$$\beta_{lg}^{obs} = \beta_{lg,\,nonenz} + \beta_{bind}^{\ddagger} \quad (1)$$

$$\beta_{lg,\,nonenz} = \beta_{lg,\,^{-}OH} + p_{xy}\Delta pK_{nuc} \quad (2)$$

$$\beta_{bind}^{\ddagger} = \beta_{bridge\ \ Zn\ \ bind}^{\ddagger} + \beta_{nonbridge\ \ Zn\ \ bind}^{\ddagger} \quad (3)$$

The interaction coefficient p_{xy} describes the change in β_{lg} with changing nucleophile strength (ΔpK_{nuc}) relative to a reference reaction (Eq. 2). The pK_a of the Ser-$O^{-}\cdots Zn^{2+}$ nucleophile in the E•S complex is estimated to be ~7.[98] Relative to a solution reaction with hydroxide ion (pK_a = 15.7) as the nucleophile and using p_{xy} = 0.019,[35] $\Delta\beta_{lg,\,nonenz} = p_{xy} \times \Delta pK_{nuc}$ = 0.019

× (7 − 15.7) = −0.17. The value of $\beta_{lg,\ ^{-}OH}$ from this work of −0.94 (see Results) gives $\beta_{lg,\ nonenz} = -0.94 + -0.17 = -1.11$ (Eq. 2).

$\beta^{\ddagger}_{bind}$ (Scheme 4) has contributions from interactions with the active site Zn^{2+} at both the bridging and nonbridging phosphate ester oxygen atoms in the transition state (Scheme 1 and Eq. 3). The bridging contribution can be estimated from the literature value[99] of $\beta^{phenolate}_{Zn\ bind}$ and the fractional effective charge in the transition state[54, 55] (β_{lg}/β_{eq}) according to:

$$\beta^{\ddagger}_{bridge\ \ Zn\ \ bind} = \beta^{phenolate}_{Zn\ \ bind} \times (\text{fractional effective charge}) \quad (4)$$

Using $\beta_{lg,\ nonenz} = -1.11$ and $\beta_{eq} = -1.73$,[56] the fractional effective charge is $\beta_{lg,\ nonenz}/\beta_{eq} = 0.64$, giving $\beta^{\ddagger}_{bridge\ Zn\ bind} = 0.36 \times 0.64 = 0.23$ (Eq. 4). $\beta^{\ddagger}_{nonbridge\ Zn\ bind}$ accounts for the change in Zn^{2+} affinity to the non-bridging oxygen atom of a phosphate diester in the transition state with the pK_a of the leaving group according to:

$$\log\ \left(K^{nonbridge}_{Zn}\right) \propto \beta^{\ddagger}_{nonbridge\ \ Zn\ \ bind}\ \ pK_{ROH} \quad (5)$$

This quantity cannot be directly measured, but it can be crudely approximated from literature data. Eq. 6 correlates the binding constants of phosphate esters to Zn^{2+} with the pK_a of the phosphate ester (pK_{ROP}).[100] Eq. 7 correlates the pK_a of phosphate diesters (pK_{ROP}) with the pK_a of the leaving group (pK_{ROH}),[56] which can be used to convert a dependence on pK_{ROP} to a dependence on pK_{ROH}. Combining Eqs. 6 and 7 gives an estimate for $\beta^{\ddagger}_{nonbridge\ Zn\ bind}$ of 0.03 (Eq. 8). Then $\beta^{\ddagger}_{bind} = \beta^{\ddagger}_{bridge\ Zn\ bind} + \beta^{\ddagger}_{nonbridge\ Zn\ bind} = 0.23 + 0.03 = 0.26$ (Eq. 3).

$$\log\ \left(K^{nonbridge}_{Zn}\right) \propto 0.35\ \ pK_{ROP} \quad (6)$$

$$pK_{ROP} \propto 0.09\ \ pK_{ROH} \quad (7)$$

$$\log\ \left(K^{nonbridge}_{Zn}\right) \propto 0.03\ \ pK_{ROH} \quad (8)$$

The contributions from binding interactions and changing nucleophile strength predict $\beta^{obs}_{lg} = \beta_{lg,\ \ nonenz} + \beta^{\ddagger}_{bind} = -1.11 + 0.26 = -0.85$ (Eq. 1) for an enzymatic transition state similar to that for phosphate diester hydrolysis in solution.

Comparison for a Monoester-like Transition State

For phosphate monoester hydrolysis, $\beta_{lg} = -1.23$.[30] Accounting for nucleophile strength from neutral water to Ser-$O^{-}\cdots Zn^{2+}$ using $p_{xy} = 0.013$[101] gives $\Delta\beta_{lg,\ nonenz} = p_{xy} \times \Delta pK_{nuc} = 0.013 \times (7 - (-1.7)) = 0.11$ and $\beta^{monoester}_{lg,\ \ nonenz} = -1.23 + 0.11 = -1.12$ (Eq. 2). From $\beta^{monoester}_{eq} = -1.35$,[56] the fractional effective charge is $\beta^{monoester}_{lg,\ \ nonenz}/\beta^{monoester}_{eq} = 0.83$. If the diester were to proceed through a transition state with similar fractional effective charge, $\beta^{diester}_{lg,\ \ nonenz}/\beta^{diester}_{eq}$ would equal 0.83. Given the value of $\beta^{diester}_{eq} = -1.73$, $\beta^{diester}_{lg,\ \ nonenz}$ would equal −1.44. For binding interactions: $\beta^{\ddagger}_{bridge\ Zn\ bind} = \beta^{phenolate}_{Zn\ bind} \times$ (fractional effective charge) = 0.36 × 0.83 = 0.30 (Eq. 4) and $\beta^{\ddagger}_{nonbridge\ Zn\ bind} = 0.03$ as described above for a diester-like transition state, assuming that there would not be drastic changes in the charge distribution at the non-bridging oxygen atoms. This term is small and unlikely to influence the outcome of this analysis. It then follows that $\beta^{\ddagger}_{bind} = 0.30 + 0.03 = 0.33$ (Eq. 3) and $\beta^{obs}_{lg} = \beta^{diester}_{lg,\ \ nonenz} + \beta^{\ddagger}_{bind} = -1.44 + 0.33 = -1.11$ (Eq. 1) for an enzymatic transition state similar to that for phosphate monoester hydrolysis in solution.

Comparison for a Triester-like Transition State

For phosphate triester hydrolysis, $\beta_{lg} = -0.99$.[79] Accounting for nucleophile strength from neutral water to Ser-O$^{-}\cdots$Zn^{2+} using $p_{xy} = 0.044$[79] gives $\Delta\beta_{lg,\ nonenz} = p_{xy} \times \Delta pK_{nuc} = 0.044 \times (7-(-1.7)) = 0.38$ and $\beta^{triester}_{lg,\ nonenz} = -0.99+0.38 = -0.61$ (Eq. 2). From $\beta^{triester}_{eq} = -1.82$,[56] the fractional effective charge is $\beta^{triester}_{lg,\ nonenz}/\beta^{triester}_{eq} = 0.34$. If the diester were to proceed through a transition state with similar fractional effective charge, $\beta^{diester}_{lg,\ nonenz}/\beta^{diester}_{eq}$ would equal 0.34. Given the value of $\beta^{diester}_{eq} = -1.73$, $\beta^{diester}_{lg,\ nonenz}$ would equal −0.59. For binding interactions: $\beta^{\ddagger}_{bridge\ Zn\ bind} = \beta^{phenolate}_{Zn\ bind} \times$ (fractional effective charge) = 0.36 × 0.34 = 0.12 (Eq. 4) and $\beta^{\ddagger}_{nonbridge\ Zn\ bind} = 0.03$ as described above for a diester-like transition state, assuming that there would not be drastic changes in the charge distribution at the non-bridging oxygen atoms. This term is small and unlikely to influence the outcome of this analysis. It then follows that $\beta^{\ddagger}_{bind} = 0.12+0.03 = 0.15$ (Eq. 3) and $\beta^{obs}_{lg} = \beta^{triester}_{lg,\ nonenz} + \beta^{\ddagger}_{bind} = -0.58+0.15 = -0.43$ (Eq. 1) for an enzymatic transition state similar to that for phosphate triester hydrolysis in solution.

Supplementary Material

Refer to Web version on PubMed Central for supplementary material.

Acknowledgements

This work was supported by a grant from the NIH to DH (GM64798). JGZ was supported in part by a Hertz Foundation Graduate Fellowship. We thank members of the Herschlag lab for comments on the manuscript.

Abbreviations

AP, *E. coli* alkaline phosphatase; PNPP, *p*-nitrophenyl phosphate; LFER, Linear Free Energy Relationship; NaMOPS, sodium 3-(*N*-morpholino)propanesulfonate; P_i, inorganic phosphate; wt, wild type; KIE, Kinetic Isotope Effect.

References

1. Coleman JE. Annu. Rev. Biophys. Biomol. Struct 1992;21:441–483. [PubMed: 1525473]
2. O'Brien PJ, Herschlag D. Biochemistry 2001;40:5691–5699. [PubMed: 11341834]
3. Jensen RA. Annu. Rev. Microbiol 1976;30:409–425. [PubMed: 791073]
4. O'Brien PJ, Herschlag D. Chem. Biol 1999;6:R91–R105. [PubMed: 10099128]
5. Palmer DRJ, Garrett JB, Sharma V, Meganathan R, Babbitt PC, Gerlt JA. Biochemistry 1999;38:4252–4258. [PubMed: 10194342]
6. Penning TM, Jez JM. Chem. Rev 2001;101:3027–3046. [PubMed: 11710061]
7. Copley SD. Curr. Opin. Chem. Biol 2003;7:265–272. [PubMed: 12714060]
8. James LC, Tawfik DS. Trends Biochem. Sci 2003;28:361–368. [PubMed: 12878003]
9. Galperin MY, Bairoch A, Koonin EV. Protein Sci 1998;7:1829–1835. [PubMed: 10082381]
10. Galperin MY, Jedrzejas MJ. Proteins 2001;45:318–324. [PubMed: 11746679]
11. Gijsbers R, Ceulemans H, Stalmans W, Bollen M. J. Biol. Chem 2001;276:1361–1368. [PubMed: 11027689]
12. Kim EE, Wyckoff HW. J. Mol. Biol 1991;218:449–464. [PubMed: 2010919]
13. Holtz KM, Stec B, Kantrowitz ER. J. Biol. Chem 1999;274:8351–8354. [PubMed: 10085061]
14. Beese LS, Steitz TA. EMBO J 1991;10:25–33. [PubMed: 1989886]
15. Steitz TA. J. Biol. Chem 1999;274:17395–17398. [PubMed: 10364165]
16. Wilcox DE. Chem. Rev 1996;96:2435–2458. [PubMed: 11848832]

17. Strater N, Lipscomb WN, Klabunde T, Krebs B. Angew. Chem. Int. Ed. Engl 1996;35:2024–2055.
18. Polanyi MZ. Elektrochem. Z 1921;27:142.
19. Pauling L. Chem. Eng. News 1946;24:1375–1377.
20. Wolfenden R. Acc. Chem. Res 1972;5:10–18.
21. Lienhard GE. Science 1973;180:149–154. [PubMed: 4632837]
22. Jencks, WP. Catalysis in Chemistry and Enzymology. Dover Publications, Inc.; New York: 1987.
23. Weiss PM, Cleland WW. J. Am. Chem. Soc 1989;111:1928–1929.
24. Hollfelder F, Herschlag D. Biochemistry 1995;34:12255–12264. [PubMed: 7547968]
25. O'Brien PJ, Herschlag D. J. Am. Chem. Soc 1999;121:11022–11023.
26. Holtz KM, Catrina IE, Hengge AC, Kantrowitz ER. Biochemistry 2000;39:9451–9458. [PubMed: 10924140]
27. O'Brien PJ, Herschlag D. Biochemistry 2002;41:3207–3225. [PubMed: 11863460]
28. Nikolic-Hughes I, Rees DC, Herschlag D. J. Am. Chem. Soc 2004;126:11814–11819. [PubMed: 15382915]
29. Kirby AJ, Jencks WP. J. Am. Chem. Soc 1965;87:3209–3216.
30. Kirby AJ, Varvoglis AG. J. Am. Chem. Soc 1967;89:415–423.
31. Hengge AC, Edens WA, Elsing H. J. Am. Chem. Soc 1994;116:5045–5049.
32. Thatcher GRJ, Kluger R. Adv. Phys. Org. Chem 1989;25:99–265.
33. Hengge AC, Onyido I. Curr. Org. Chem 2005;9:61–74.
34. Kirby AJ, Younas M. J. Chem. Soc. (B) 1970:1165–1172.
35. Kirby AJ, Younas M. J. Chem. Soc. (B) 1970:510–513.
36. Hengge AC, Cleland WW. J. Am. Chem. Soc 1991;113:5835–5841.
37. Hengge AC, Tobin AE, Cleland WW. J. Am. Chem. Soc 1995;117:5919–5926.
38. More O'Ferrall RA. J. Chem. Soc. (B) 1970:274–277.
39. Jencks WP. Chem. Rev 1972;72:705–718.
40. Breslow R, Katz I. J. Am. Chem. Soc 1968;90:7376–7377.
41. Hall AD, Williams A. Biochemistry 1986;25:4784–4790. [PubMed: 3533141]
42. Han R, Coleman JE. Biochemistry 1995;34:4238–4245. [PubMed: 7703237]
43. Jencks WP. Chem. Rev 1985;85:511–527.
44. Herschlag D, Jencks WP. Biochemistry 1990;29:5172–5179. [PubMed: 2378873]
45. Herschlag D, Piccirilli JA, Cech TR. Biochemistry 1991;30:4844–4854. [PubMed: 2036355]
46. Zhang YL, Hollfelder F, Gordon SJ, Chen L, Keng YF, Wu L, Herschlag D, Zhang ZY. Biochemistry 1999;38:12111–12123. [PubMed: 10508416]
47. Williams A. Adv. Phys. Org. Chem 1992;27:1–55.
48. Although β_{lg} reflects the extent of bonding, it is not a direct measurement of bond order. Solvent interactions, hydrogen bonding, general acid/general base catalysis, and metal ion interactions can also affect the observed value of β_{lg}.
49. Chin J, Banaszczyk M, Jubian V, Zou X. J. Am. Chem. Soc 1989;111:186–190.
50. Williams NH, Cheung W, Chin J. J. Am. Chem. Soc 1998;120:8079–8087.
51. Liao XM, Anjaneyulu PSR, Curley JF, Hsu M, Boehringer M, Caruthers MH, Piccirilli JA. Biochemistry 2001;40:10911–10926. [PubMed: 11551186]
52. Ba-Saif SA, Davis AM, Williams A. J. Org. Chem 1989;54:5483–5486.
53. Williams NH, Wyman P. Chem. Commun 2001:1268–1269.
54. Leffler JE. Science 1953;117:340–341. [PubMed: 17741025]
55. Williams A. Acc. Chem. Res 1984;17:425–430.
56. Bourne N, Williams A. J. Org. Chem 1984;49:1200–1204.
57. Jencks, WP.; Regenstein, J. Ionization Constants of Acids and Bases.. In: Fasman, GD., editor. Handbook of Biochemistry and Molecular Biology. CRC; Cleveland, OH: 1976.
58. Bolton PD, Ellis J, Hall FM. J. Chem. Soc. (B) 1970:1252–1255.

59. Chaidaroglou A, Brezinski DJ, Middleton SA, Kantrowitz ER. Biochemistry 1988;27:8338–8343. [PubMed: 3072019]
60. Bernasconi CF. Adv. Phys. Org. Chem 1992;27:119–238.
61. See references in O'Brien and Herschlag, 1999 and Nikolic-Hughes, Rees, and Herschlag, 2004.[25, 28]
62. Rajca A, Rice JE, Streitwieser A, Schaefer HF. J. Am. Chem. Soc 1987;109:4189–4192.
63. Horn H, Ahlrichs R. J. Am. Chem. Soc 1990;112:2121–2124.
64. Mildvan AS. Proteins 1997;29:401–416. [PubMed: 9408938]
65. Hengge AC. Acc. Chem. Res 2002;35:105–112. [PubMed: 11851388]
66. Grzyska PK, Kim Y, Jackson MD, Hengge AC, Denu JM. Biochemistry 2004;43:8807–8814. [PubMed: 15236589]
67. McCain DF, Grzyska PK, Wu L, Hengge AC, Zhang ZY. Biochemistry 2004;43:8256–8264. [PubMed: 15209522]
68. Hengge AC, Martin BL. Biochemistry 1997;36:10185–10191. [PubMed: 9254616]
69. Hoff RH, Mertz P, Rusnak F, Hengge AC. J. Am. Chem. Soc 1999;121:6382–6390.
70. Du XL, Black GE, Lecchi P, Abramson FP, Sprang SR. Proc. Natl. Acad. Sci. U.S.A 2004;101:8858–8863. [PubMed: 15178760]
71. Kim K, Cole PA. J. Am. Chem. Soc 1997;119:11096–11097.
72. Kim K, Cole PA. J. Am. Chem. Soc 1998;120:6851–6858.
73. Paoli P, Cirri P, Camici L, Manao G, Cappugi G, Moneti G, Pieraccini G, Camici G, Ramponi G. Biochem. J 1997;327:177–184. [PubMed: 9355750]
74. Gerratana B, Frey PA, Cleland WW. Biochemistry 2001;40:2972–2977. [PubMed: 11258909]
75. Cassano AG, Anderson VE, Harris ME. Biochemistry 2004;43:10547–10559. [PubMed: 15301552]
76. Caldwell SR, Raushel FM, Weiss PM, Cleland WW. Biochemistry 1991;30:7444–7450. [PubMed: 1649629]
77. Caldwell SR, Newcomb JR, Schlecht KA, Raushel FM. Biochemistry 1991;30:7438–7444. [PubMed: 1649628]
78. Hong SB, Raushel FM. Biochemistry 1996;35:10904–10912. [PubMed: 8718883]
79. Khan SA, Kirby AJ. J. Chem. Soc. (B) 1970:1172–1182.
80. Liu SJ, Lu ZB, Jia Y, Dunaway-Mariano D, Herzberg O. Biochemistry 2002;41:10270–10276. [PubMed: 12162742]
81. Choe JY, Iancu CV, Fromm HJ, Honzatko RB. J. Biol. Chem 2003;278:16015–16020. [PubMed: 12595528]
82. Lahiri SD, Zhang GF, Dunaway-Mariano D, Allen KN. Science 2003;299:2067–2071. [PubMed: 12637673]
83. Leiros I, McSweeney S, Hough E. J. Mol. Biol 2004;339:805–820. [PubMed: 15165852]
84. Blackburn GM, Williams NH, Gamblin SJ, Smerdon SJ. Science 2003;301:1184c. [PubMed: 12947182]
85. Allen KN, Dunaway-Mariano D. Science 2003;301:1184d.
86. Yarnell A. Chem. Eng. News 2003;81:30–31.
87. Webster CE. J. Am. Chem. Soc 2004;126:6840–6841. [PubMed: 15174833]
88. Tremblay LW, Zhang G, Dai J, Dunaway-Mariano D, Allen KN. J. Am. Chem. Soc 2005;127:5298–5299. [PubMed: 15826149]
89. Berti PJ, Tanaka KSE. Adv. Phys. Org. Chem 2002;37:239–314.
90. Schramm VL. Acc. Chem. Res 2003;36:588–596. [PubMed: 12924955]
91. Amyes TL, Jencks WP. J. Am. Chem. Soc 1989;111:7900–7909.
92. Banait NS, Jencks WP. J. Am. Chem. Soc 1991;113:7951–7958.
93. O'Brien PJ, Herschlag D. J. Am. Chem. Soc 1998;120:12369–12370.
94. Nikolic-Hughes I, O'Brien PJ, Herschlag D. J. Am. Chem. Soc 2005;127:9314–9315. [PubMed: 15984827]

95. Cassano AG, Anderson VE, Harris ME. J. Am. Chem. Soc 2002;124:10964–10965. [PubMed: 12224928]

96. Lad C, Williams NH, Wolfenden R. Proc. Natl. Acad. Sci. U.S.A 2003;100:5607–5610. [PubMed: 12721374]

97. Gill SC, von Hippel PH. Anal. Biochem 1989;182:319–326. [PubMed: 2610349]

98. The pK_a of Ser-$O^{-}\cdots Zn^{2+}$ in the E•S complex has not been experimentally determined. The pK_a in the free enzyme is ≤5.5,[27] and binding of a negatively charged substrate is expected to increase the pK_a. Using a pK_a of 4 or of 9, the pK_a of a Zn^{2+}-bound water,[102] does not significantly alter the results of this analysis and does not affect the conclusions drawn

99. Postmus C, Magnusson LB, Craig CA. Inorg. Chem 1966;5:1154–1157.

100. Massoud SS, Sigel H. Inorg. Chem 1988;27:1447–1453. The correlation of binding constants of phosphate esters to Zn^{2+} with the pK_a of the phosphate ester (Eq. 5) was determined for phosphate monoesters. We assume that this correlation also holds for diesters

101. Herschlag D, Jencks WP. J. Am. Chem. Soc 1989;111:7587–7596.

102. Baes, CF., Jr.; Mesmer, RE. The Hydrolysis of Cations. Wiley; New York: 1976.

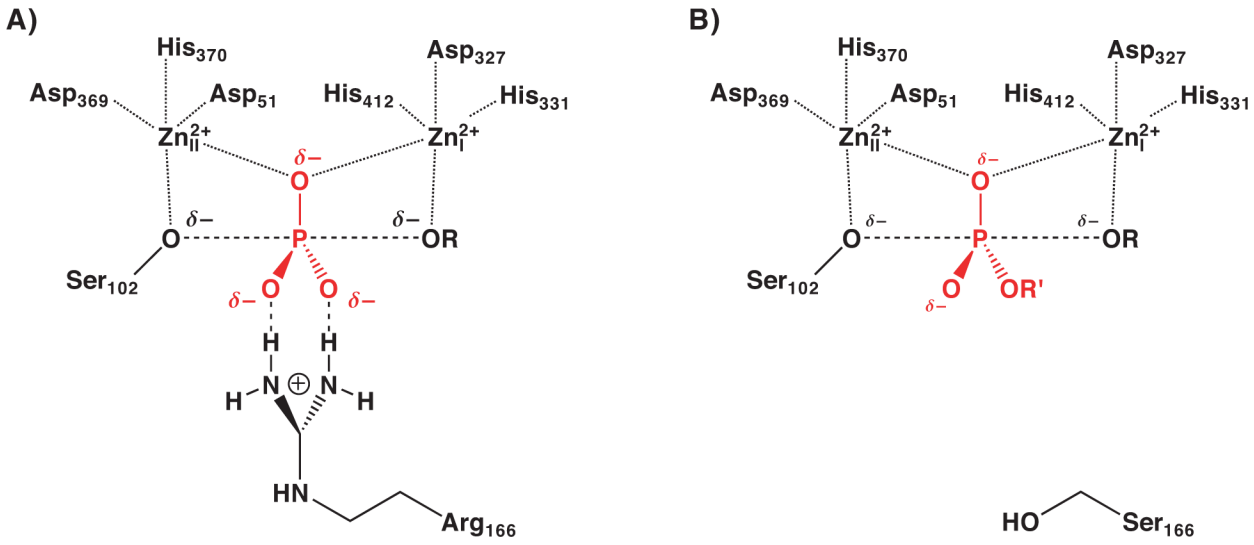

Scheme 1.

Proposed AP active site interactions of wt AP with a phosphate monoester substrate (A) and of R166S AP with a phosphate diester substrate (B).[12, 13] In both cases the reaction is depicted in terms of a transition state representation with partial bond formation and bond cleavage. No information about bond orders and bond lengths is conveyed in this schematic.

A) Phosphate monoester hydrolysis through a loose transition state

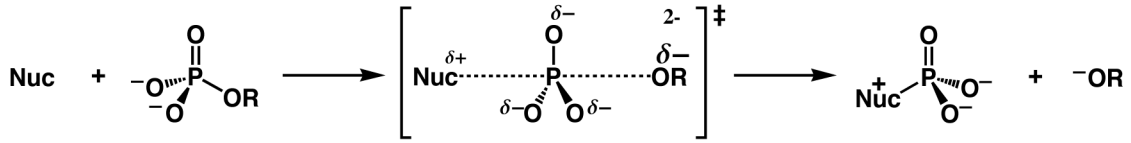

B) Phosphate diester hydrolysis through a roughly synchronous transition state

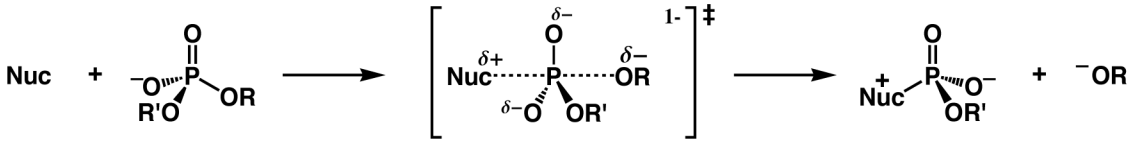

Scheme 2.
Non-enzymatic transition states for reactions of phosphate monoesters and diesters.

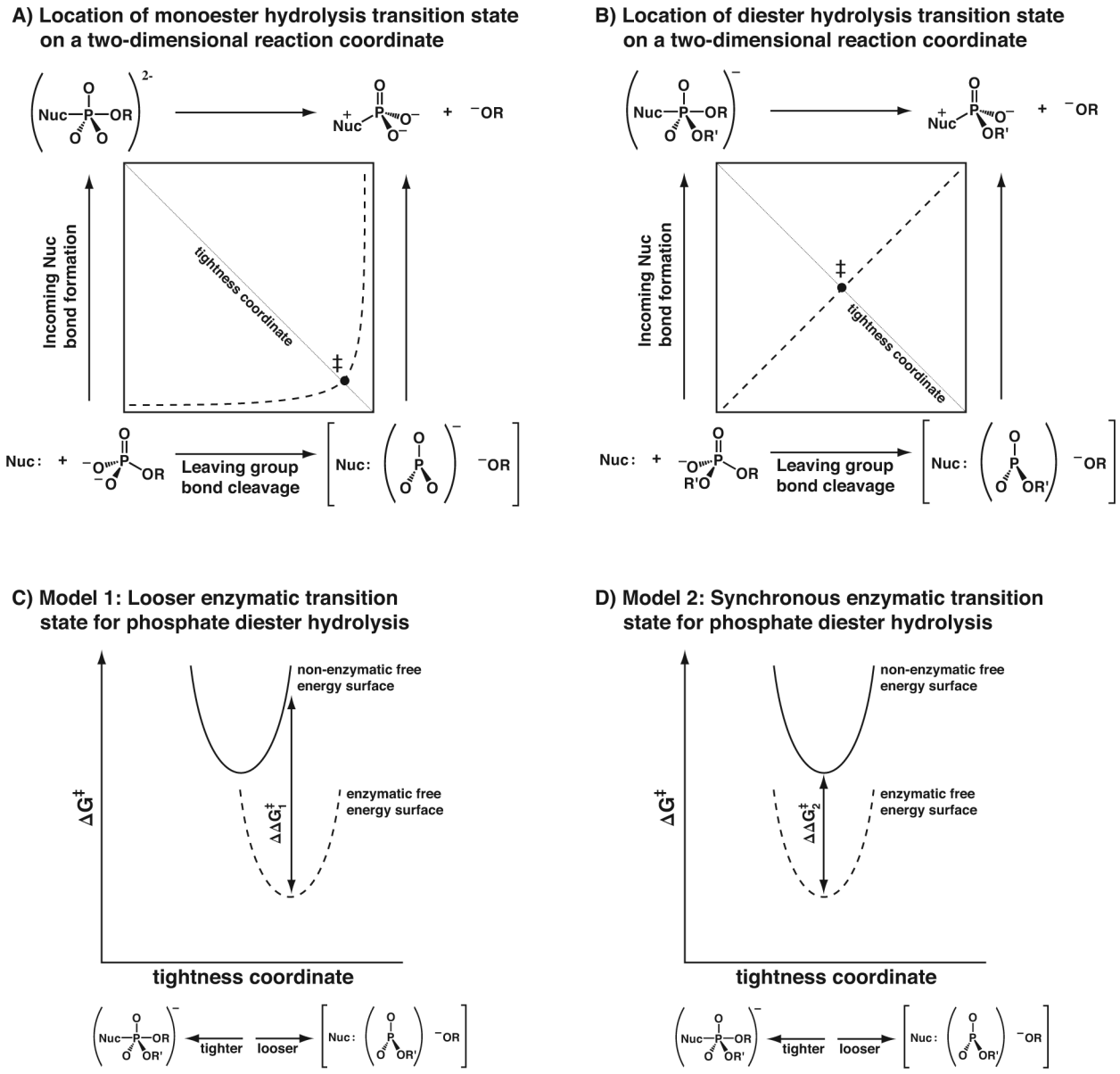

Figure 1.

Reaction coordinate diagrams for phosphate ester hydrolysis in solution. A, B) Two-dimensional reaction coordinate diagrams for phosphate monoester (A) and diester (B) hydrolysis. In both cases, a symmetrical transition state is depicted for simplicity. The transition state can be asymmetrical for nucleophiles and leaving groups with different pK_a values, atom identities, or charges.[43] C, D) Cross sections of the free energy surface along the tightness coordinate showing the relationship between the solution and enzymatic transition states. In Model 1, AP catalyzes phosphate diester hydrolysis through a looser transition state than that in solution (C). In Model 2, AP catalyzes phosphate diester hydrolysis through a synchronous transition state similar to that in solution (D).

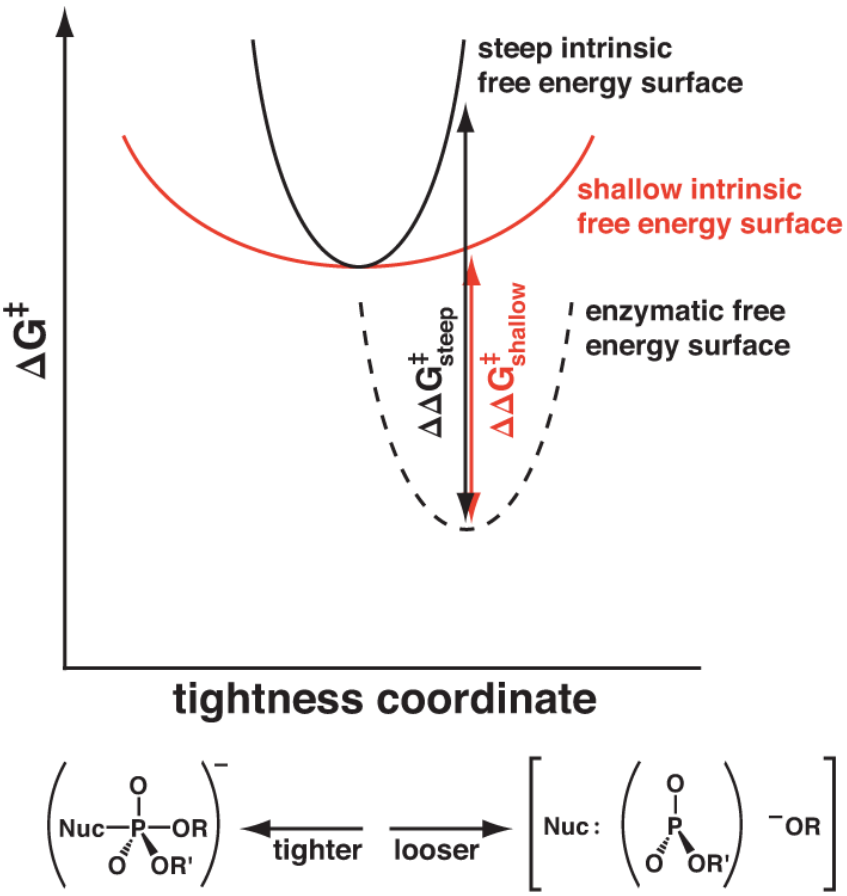

Figure 2.

The energy required to stabilize an altered transition state and provide a given amount of catalysis depends on the steepness of the intrinsic free energy surface. More energetic stabilization is required for a steep intrinsic free energy surface than a shallow surface $\left(|\Delta\Delta G^{\ddagger}_{Step}|>|\Delta\Delta G^{\ddagger}_{Shallow}|\right)$. The steepness of the intrinsic free energy surface refers to how energetically costly it is to vary the tightness of the transition state.

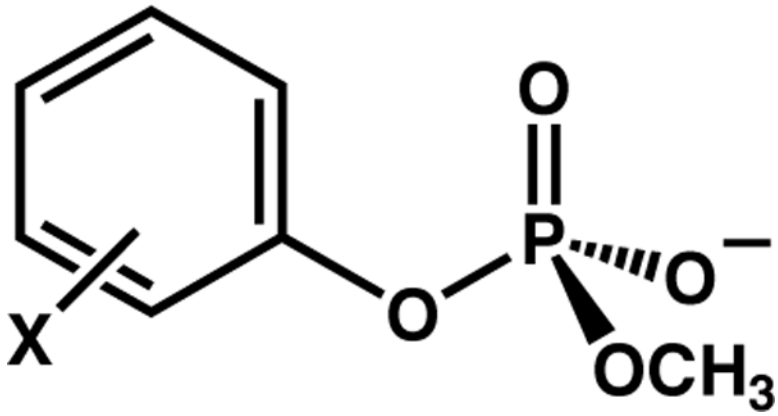

Scheme 3.
Methyl Phenyl Phosphate Diesters

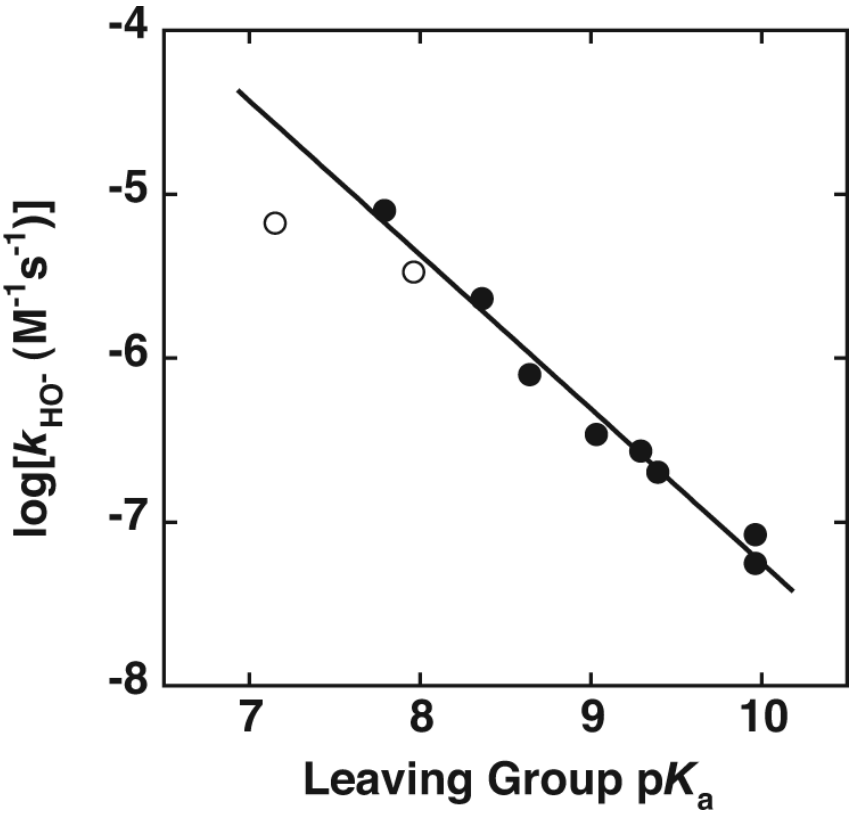

Figure 3.

Leaving group dependence for attack of hydroxide ion on methyl phenyl phosphate diesters. Values of k_{HO^-} ($M^{-1}s^{-1}$) are from Table 1. The solid line is a least-squares fit to the data with a slope (β_{lg}) of −0.94 ± 0.05. Rate constants for compounds with 4-nitrophenyl and 4-cyano substituents (open circles) were omitted from the fit based on literature precedent for the occurrence of outliers due to resonance effects (see Supporting Information).

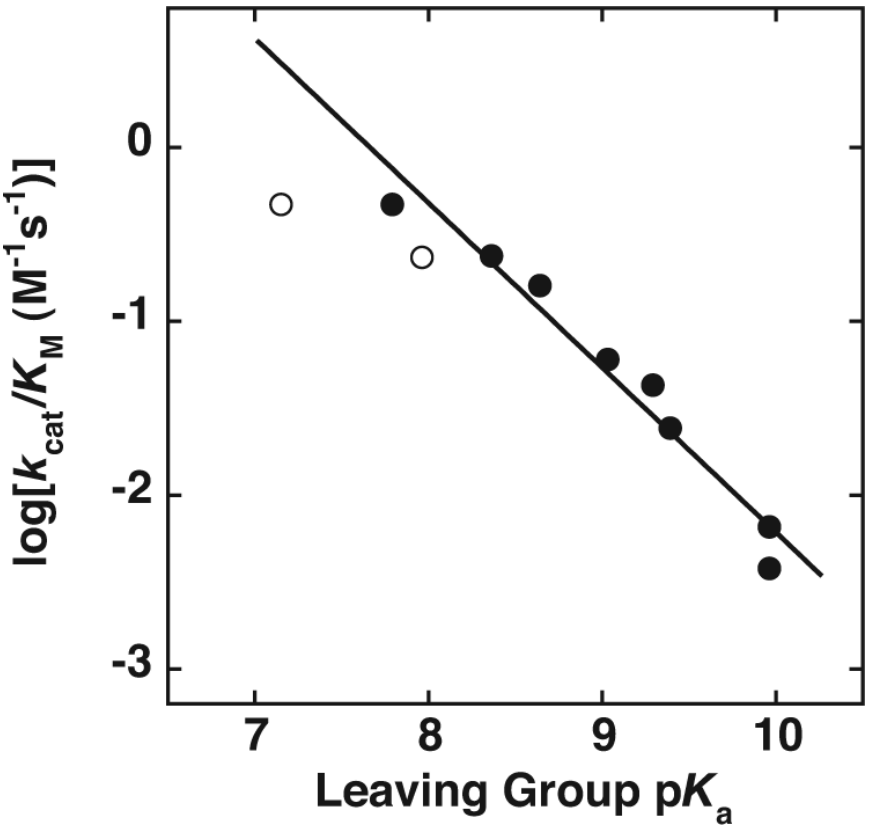

Figure 4.

R166S AP-catalyzed hydrolysis of methyl phenyl phosphate diesters. Values of k_{cat}/K_M ($M^{-1}s^{-1}$) are from Table 1. The solid line is a least-squares fit to the data with a slope (β_{lg}) of -0.95 ± 0.08. Rate constants for compounds with 4-nitrophenyl and 4-cyano substituents (open circles) were omitted from the fit based on previous results with phosphorothioate and sulfate esters in which leaving groups with these substituents were unambiguous outliers.[24, 26, 28]

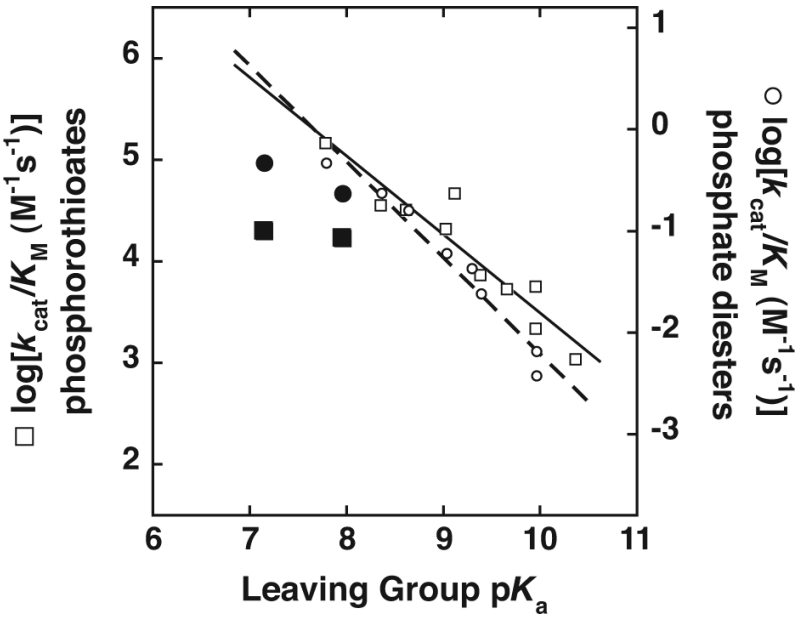

Figure 5.

Deviations from the methyl phenyl phosphate diester LFER are small. LFERs for wt AP-catalyzed hydrolysis of phenyl phosphorothioates (□,■)[24] and R166S AP-catalyzed hydrolysis of methyl phenyl phosphate diesters (○,•) are superimposed. The lines are least-squares fits to the data (open symbols) with a slope (β_{lg}) of −0.77 ± 0.09 for phenyl phosphorothioates (solid line) and −0.95 ± 0.08 for phosphate diesters (dotted line). Rate constants for compounds with 4-nitrophenyl and 4-cyano substituents (filled symbols) were not included in either fit. These leaving groups significantly deviate from the phosphorothioate LFER, but show smaller deviations from the diester LFER.

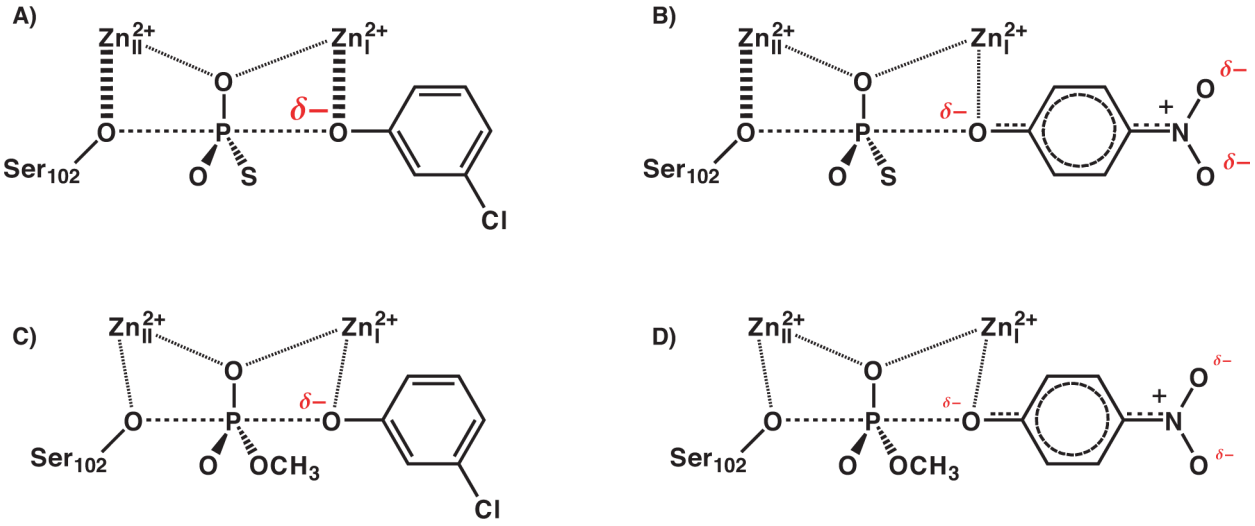

Figure 6.

Resonance effects weaken interactions with active site Zn^{2+} for a loose transition but have a smaller effect on a tight transition state. A) There is a large amount of charge buildup on the bridging oxygen in the transition state for hydrolysis of phenyl phosphorothioates (3-chlorophenyl phosphorothioate is arbitrarily chosen as an example). B) 4-nitro and 4-cyano groups delocalize electron density buildup at the bridging oxygen and weaken the interaction with the active site Zn_1^{2+}, leading to a smaller than expected overall rate enhancement. C) In the tighter transition state for the phosphate diester hydrolysis reaction, there is less charge buildup at the bridging oxygen. Interactions with Zn_1^{2+} may be weaker and therefore less important for the rate enhancement. D) 4-Nitro and 4-cyano groups delocalize charge, but if the interaction with Zn_1^{2+} is weaker, the deviation from the expected rate enhancement will be smaller.

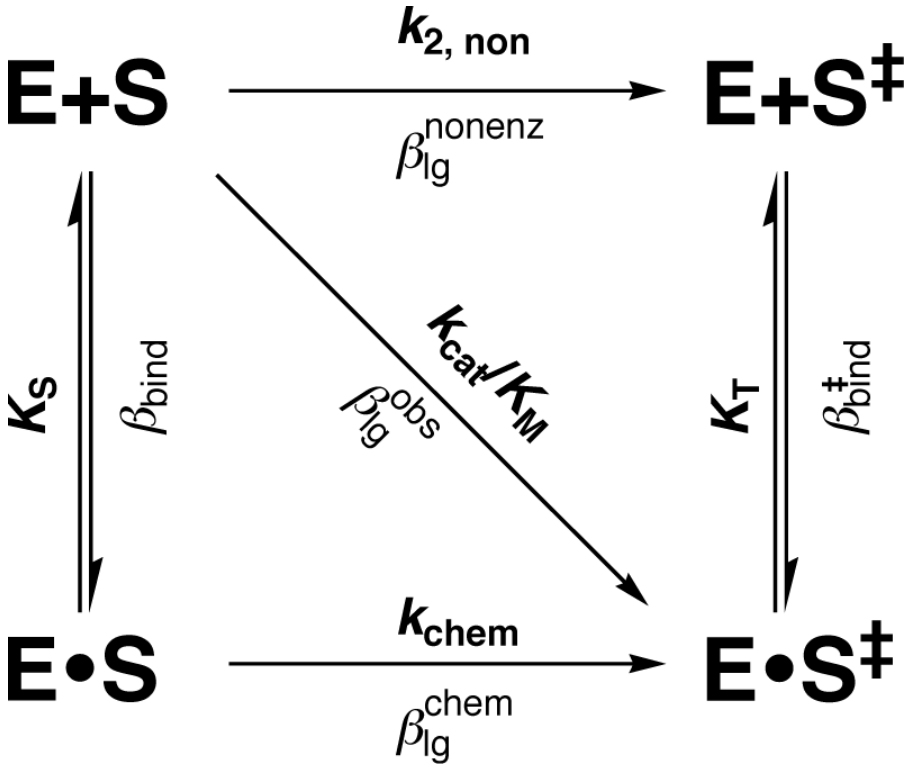

Scheme 4.
Binding interactions affect β_{lg}.

Table 1

Rate constants for enzymatic methyl phenyl phosphate diester hydrolysis at 25 °C, pH 8.0 (k_{cat}/K_M) and for the non-enzymatic reaction with hydroxide at 42 °C (k_{HO^-}).[a]

Phenyl substituent	Phenol pK_a	k_{cat}/K_M ($M^{-1}s^{-1}$)	k_{HO^-} ($M^{-1}s^{-1}$)
4-nitro	7.14	$(4.8 \pm 0.1) \times 10^{-1}$	$(6.9 \pm 0.3) \times 10^{-6}$
4-chloro-3-nitro	7.78	$(4.8 \pm 0.8) \times 10^{-1}$	$(8.2 \pm 0.3) \times 10^{-6}$
4-cyano	7.95	$(2.4 \pm 0.2) \times 10^{-1}$	$(3.5 \pm 0.2) \times 10^{-6}$
3-nitro	8.35	$(2.4 \pm 0.1) \times 10^{-1}$	$(2.4 \pm 0.1) \times 10^{-6}$
3,4-dichloro	8.63	$(1.7 \pm 0.1) \times 10^{-1}$	$(8.2 \pm 0.5) \times 10^{-7}$
3-chloro	9.02	$(6.2 \pm 0.2) \times 10^{-2}$	$(3.5 \pm 0.4) \times 10^{-7}$
3-fluoro	9.28	$(4.4 \pm 1.0) \times 10^{-2}$	$(2.8 \pm 0.2) \times 10^{-7}$
4-chloro	9.38	$(2.5 \pm 1.1) \times 10^{-2}$	$(2.1 \pm 0.1) \times 10^{-7}$
4-fluoro	9.95	$(6.8 \pm 0.1) \times 10^{-3}$	$(8.6 \pm 1.1) \times 10^{-8}$
Parent	9.95	$(3.9 \pm 0.1) \times 10^{-3}$	$(5.8 \pm 0.3) \times 10^{-8}$

[a] pK_a values are from Jencks and Regenstein[57] except 4-chloro-3-nitro, which was calculated from the increments of the 4-chloro and 3-nitro groups, and 3,4-dichloro.[58] The uncertainty is the standard deviation from at least six measurements.

Table 2

Comparison of observed and predicted values of β_{lg} for AP-catalyzed reactions.[a]

Predicted Transition State Structure	β_{lg}^{pred}	β_{lg}^{obs}
Monoester Reaction[b]		
Loose	−0.69	**−0.85 ± 0.13**
Synchronous	−0.25	
Tight	0.06	
Diester Reaction[c]		
Loose	−1.11	**−0.95 ± 0.08**
Synchronous	−0.85	
Tight	−0.43	

[a] Although similar, the observed values of β_{lg} for the monoester and diester reactions are not directly comparable. For transition states with identical axial bonding, predicted values of β_{lg} for the monoester reaction are smaller in magnitude than those for the diester reaction because of differences in the values of β_{eq} and in estimates for the strength of the interaction between the leaving group oxygen and the Zn^{2+} ion in the transition state.

[b] Values of β_{lg} for the monoester reaction with wt AP are from O'Brien and Herschlag, 2002.[27] The predicted values take into account changes in nucleophile strength and interactions with active site Zn^{2+} ions. Interactions with Arg166 were not taken into account because mutation of Arg166 to Ser has no significant effect on the value of β_{lg}.[25, 26]

[c] The predicted values for the diester reaction were obtained analogous to those for the monoester reaction as described in the Methods section.